Experimental Study of the Wetting of Fibers

Mamdouh T. Ghannam and M. Nabil Esmail
Dept. of Chemical Engineering, University of Saskatchewan, Saskatoon, Canada S7N 0W0

During the coating process, liquid displaces air from the surface of the solid substrate at the three-phase contact line (that is, line of contact between air, liquid, and solid). If we look through an optical microscope, we will see that the liquid/air interface intersects the solid substrate at a specific angle. We call this angle the apparent dynamic contact angle. At a yet smaller scale, when the roughness of the solid surface can be seen, the liquid/air interface may intersect the surface with another "true" angle of contact. Meanwhile, the distance along the substrate surface, between the three-phase contact line and the horizontal level of the free surface, is usually called the interfacial displacement depth X_d. Static contact angles, achieved under stagnation conditions have been extensively studied. Dynamic contact angles, interfacial displacement depths, and the criteria for air entrainment in wetting have been studied for dry continuous tapes (Perry, 1967; Burley and Jolly, 1984; Gutoff and Kendrick, 1982).

In general, apparent dynamic contact angles are associated with moving wetting lines, and significantly differ from their static values. They increase with the speed of the substrate. At a certain velocity the three-phase contact line ceases to be a straight, stable, and horizontal line. Instead, V-shaped patterns start to form at different locations of the line. Further increase in the coating speed leads to the appearance of tiny air bubbles in the coating layer. It has been shown that these bubbles break off from the tips of the V-shapes (Blake and Ruschak, 1979). Finally, at a higher speed of coating, a continuous air sheet is entrained in the coating liquid and the liquid ceases to wet the surface. The dynamic contact angle approaches 180° in these stages.

Dynamic contact angles and entrainment criteria are important factors in fiber coating. In a coating process, the fiber usually passes through a cup filled with the coating liquid. The coated fiber leaves the cup from a hole at its bottom. In fiber-optics production, silicone is frequently used as a coating liquid. At low fiber speeds, the three-phase contact line is stable, and complete wetting is achieved. Tiny air bubbles are entrained into the coating layer at rather low speeds in the case of high viscosity liquids such as silicone. Air bubbles are entrained by silicone at a fiber speed of few centimeters per second. Less viscous liquids entrain air bubbles at substrate speeds of a hundred centimeters per second or more. It is well known that the capillary number $Ca = \mu V/\sigma$ is an important dimensionless group in liquid coating phenomena (Esmail and Hummel, 1975) and particularly in establishing criteria for the onset of air entrainment. In addition, dynamic contact angles are an important parameter in liquid coating processes. Their importance arises from the need to establish mathematical models of these processes and their numerical solution. Their values are used as boundary conditions in coating models and correspond to the apparent contact angles which we defined earlier.

Experimental work in the wetting phenomena in liquid coating covers some basic ideas, such as the measurements of dynamic contact angles, interfacial displacement depths, and the criteria for air entrainment by substrates. In previous work, we studied the air entrainment phenomena in liquid coating systems using dry and pre-wet roll-coaters (Esmail and Ghannam, 1990; Ghannam and Esmail, 1992). For a more detailed description of previous work, see, for example, Blake (1988) or Ghannam (1991).

In this work, we investigated the basic parameters of wetting for a fiber-coating system. The purpose was to measure the dynamic contact angle, interfacial displacement depth, and the critical speed of air entrainment for the fiber system, and to compare these measurements with measurements previously obtained for wetting systems which use other substrate geometries, such as a dry tape, a dry roll-coater, and a pre-wet roll-coater. We concluded that pre-wetting influences values of dynamic contact angles more than the geometry of the substrate. The critical speed of air entrainment is not influenced by the geometry of the substrate and is influenced by the surface tension force. The angle at which the fiber plunges into the liquid has no effect.

Experimental Work

The experimental system consists of a transparent plexiglass tank with dimensions 25 × 15 × 10 cm. The tank allows good observation from all sides. Plastic Monofilament fiber line served as a continuous solid substrate passing through different glycerol solutions. The fiber line had a good tensile strength

Correspondence concerning this article should be addressed to M. Nabil Esmail.

Table 1. Dimensions of the Tested Fiber Lines

Fiber Line Specification	Diameter, cm
10 lb (4.5 kg) test/force	0.0330
20 lb (9.1 kg) test/force	0.0483
30 lb (13.6 kg) test/force	0.0584
40 lb (18.2 kg) test/force	0.0711

suitable for the tension expected in the line. It also was moisture resistant. Four different diameters of fiber line were examined. Their dimensions are listed in Table 1. The fiber line was pulled by a variable speed motor. The substrate constant speed was calculated from the measurement of revolutions per minute. A high precision Computak Tachometer was used in these measurements. Thirteen different glycerol solutions with different physical properties were tested in the experiments. Viscosities and densities were measured by a Brookfield viscometer and pycnometers respectively at room temperature. Surface tension coefficients were determined by the Fisher Surface Tensiomat which is based on the platinum-iridium ring principle of du Nouy. The physical properties of the solutions are listed in Table 2. Glycerol solutions are clear and transparent. This makes marker particles or dye traces necessary for better visibility. Methylene blue dye powder was used to enhance and contrast the visibility of the liquid/air interface in contact with the solid substrate.

The entry angle α of the fiber line was measured from the horizontal position. Its effect on the critical velocity of air entrainment was studied by varying its value from 60° to 120° in 10° increments. A still macrophotography system was used to record data for the contact angles θ_s and θ and the interfacial displacement depth. This system included a Nikon F3 35 mm camera with a 50 mm F11.8 lens in the reverse position, PB-6 bellows focusing attachment, and PB-6E extension bellows. A reproduction rate of 8× at a working distance of about 4 cm, was achieved. Illumination for macrophotography was provided by an arc lamp source. The system consists of a power supply, a lamp housing with condensing lens, and a 200 watt mercury lamp. A digitizer-microcomputer system was used to measure the dynamic contact angles and the interfacial displacement depth. A slide projector was used to magnify and provide the image to the digitizer. In all our experiments, the requirement was to observe the liquid interface in the vicinity of the dynamic contact line. The size of this area is in the neighborhood of a few millimeters. Magnification was necessary for clear observation. A Cycloptic Stereoscopic Microscope was used. The microscope range of magnification extended to 40×.

Table 2. Physical Properties of Test Liquids

Solution	Density kg/m^3	Surface Tension mN/m	Viscosity mPa·s	N_{pp}
1	1,256.0	63.4	866.6	17.277
2	1,254.0	63.4	696.5	7.223
3	1,254.0	64.0	598.4	3.825
4	1,251.6	64.7	493.8	1.720
5	1,249.3	65.5	403.9	0.743
6	1,239.6	66.3	253.8	0.196
7	1,234.2	66.5	181.1	0.039
8	1,222.4	67.4	75.2	0.010
9	1,223.5	67.3	89.3	0.002
10	1,257.1	64.0	910.7	20.468
11	1,250.4	66.4	557.5	2.588
12	1,245.6	66.6	395.0	0.649
13	1,220.9	68.3	114.5	0.004

Before the experimental system was turned on, we had to follow certain precautions in order to get reliable experimental data. First, the liquid tank was cleaned with potable water followed by distilled water. Acetone was used to dry off the liquid tank from traces of water. Then the liquid tank was filled with the test solution to a certain height and the solid substrate was adjusted to the required angle. We allowed the liquid in the tank sufficient time to get rid of air bubbles produced through filling the tank. A number of supporting points guided the solid substrate and a steady speed motor was used. This eliminated surface disturbances at the plunging point. The liquid bath temperature was measured at the beginning of each run. Before recording the behavior of the intersection of the air/liquid interface with the solid substrate on the photofilm, the dynamic behavior of the three-phase contact line was observed by the microscope to determine the critical air entrainment velocity. Then, the light system was turned on to reach its full intensity and we recorded the static condition photographically. The motor was turned on to record the dynamic meniscus behavior for various substrate speeds by adjusting the gear box until we reached the air entrainment velocity. The inclination of the fiber line was then adjusted to investigate another entry angle. The liquid was then drained out of the tank, and the tank was washed and dried before the investigation of another liquid.

Results and Discussion

This system was designed to study the hydrodynamics of the wetting of a fiber line passing through glycerol solutions at different angles of entry α and to compare the results with previous experimental data obtained from continuous tapes and rotating rollers in the cases of dry and pre-wet entry. We used a fiber line with a diameter equal to 0.033 cm for all measurements, except those concerned with the study of the effect of fiber diameter.

Measurements of the apparent dynamic angles were made for glycerol solutions with physical properties' number in the range $0.01 < N_{pp} < 17.277$. With increasing substrate velocity, apparent dynamic contact angles increase rapidly from their static values, forming the nonlinear relationship $\theta = f(V)$. For the same substrate velocity these angles increase with the physical properties' number N_{pp}. Similar relationships $\theta = f(V)$ were obtained for dry-entry tapes by Gutoff and Kendrick (1982), dry-entry rotating rollers by Esmail and Ghannam (1990), and pre-wet rotating rollers by Ghannam and Esmail (1992). The growth of the dynamic contact angle (Figure 1) from its static value manifested the same trend in all the mentioned systems. However, the angle for a pre-wet roll-coating system was significantly lower than its counterparts for dry-entry fibers, tapes and rollers, for the same substrate speed. We can conclude that pre-wetting has much more impact on the value of the dynamic contact angle than the geometry of the substrate.

According to the Buckingham Pi theorem (Shames, 1962), the maximum number of independent dimensionless groups which govern a system is equal to the number of parameters

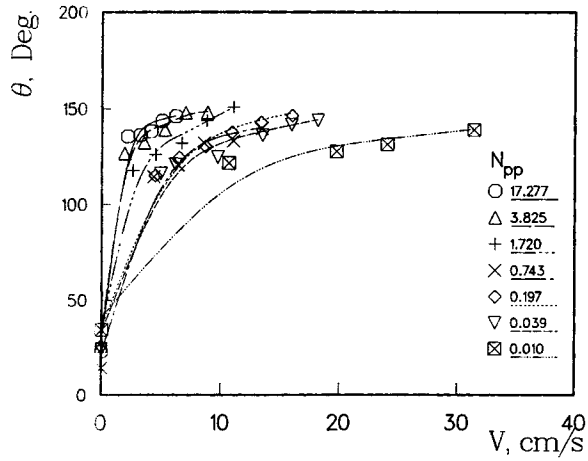

Figure 1. Dynamic contact angle vs. substrate velocity for fiber diameter = 0.033 cm.

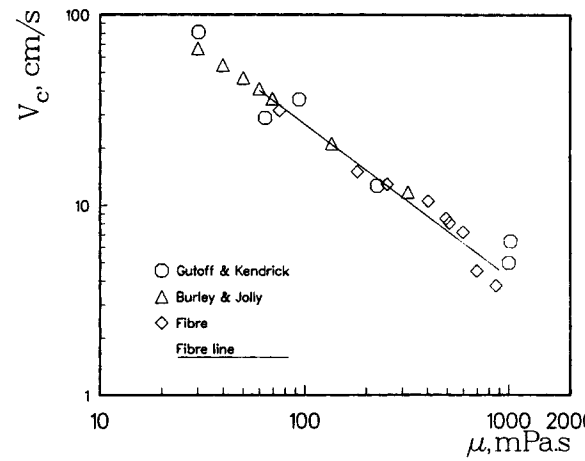

Figure 2. Critical velocity vs. liquid viscosity.

less the number of primary dimensions. The parameters are six: density, viscosity, surface tension, gravity, coating speed, and a characteristic length. The primary dimensions are three: mass, length, and time. Therefore, there exist three independent dimensionless groups. There are two possible choices for a characteristic length of the coating problem. At very low capillary numbers the capillary length $L_c=(\sigma/\rho g)^{0.5}$, which is a measure of the capillary rise of this liquid at static conditions, is a reasonable choice. At moderate to high capillary numbers it is also possible to use the Deryagin length $L_d=(\mu V/\rho g)^{0.5}$ as a characteristic value.

$$Ca=\mu V/\sigma=(\mu V/\rho g)/(\sigma/\rho g)=L_d^2/L_c^2 \tag{1}$$

Under the experimental conditions of this study, the value of capillary number Ca is less than 1. Therefore, the capillary rise can be used as a characteristic length. Consequently, the following correlations can be obtained (Esmail and Ghannam, 1990):

$$Bo=1 \tag{2}$$

$$\theta=F(Ca, N_{pp}) \tag{3}$$

Rillaerts and Joos (1980) measured the apparent dynamic contact angles using a horizontal capillary. They concluded that the dynamic contact angle was influenced only by the capillary number. Burley and Jolly (1984) also reported their measurements of the dynamic contact angle as a function of only the capillary number. The system used in their experiments was plunging continuous tapes in semi-industrial scale. Meanwhile, Gutoff and Kendrick (1982) using gelatin-coated tape entering a pool of liquid, noticed that more variables than just the capillary number were needed to define the contact angle. Measurements of dynamic contact angles for plunging dry fibers support the relationship in Eq. 3. A similar conclusion was reached by Esmail and Ghannam (1990) for a dry-entry rotating roller. It must be noted however that Burley and Jolly (1984) used liquids in the range $10^{-6}<N_{pp}<0.0035$ whereas Gutoff and Kendrick (1982) used liquids in the range $10^{-10}<N_{pp}<100$. The range of liquids used in our experiments was $0.004<N_{pp}<17.3$.

In each run, we recorded the capillary rise at static conditions and the values of interfacial displacement depth at different substrate velocities. This was done by processing the image provided by a slide projector to the digitizer-microcomputer system. Results were obtained for the whole range of $N_{pp}=17.277$ to 0.01. We found that the linear velocity of the fiber influenced the interfacial displacement depth in the same manner it influenced the apparent dynamic contact angle. The relationships of $X_d=f(V)$ for the fiber line were compared with similar relationships for other substrate geometries. The comparison showed that the values of X_d for rotating rollers in pre-wet entry were much lower than those for tapes, fibers, and rotating rollers in dry entry. This is entirely due to the fact that in the case of rotating rollers in pre-wet entry the roller was covered by a thin liquid layer when it entered through the liquid surface in the reservoir. However, the values of X_d for the fiber line and the dry rotating roller were very close. The experimental data of Burley and Kennedy (1976) showed values for the interfacial displacement depths which were slightly higher than those for the fibers and the rotating rollers.

In a wetting process when the surface is moving with a certain speed from air to the liquid phase, tiny visible air bubbles start to appear in the liquid phase at a certain critical speed. The entrainment of air occurs when the three-phase contact line is broken in one or more v-shaped formations and the air bubbles break off their vertices. It has been previously established that critical speed of air entrainment is a strong function of liquid viscosity. Figure 2 displays the measured critical speeds for the Monofilament fiber line as a function of liquid viscosity. Our measurements agree with similar measurements made for the wetting of continuous dry tapes by Gutoff and Kendrick (1980) and Burley and Jolly (1984). Measurements for the fiber line produced the regression line shown in Figure 2. This line can be expressed by the relationship:

$$V_c=1{,}083\ \mu^{-0.804} \quad r=0.94 \tag{4}$$

where V_c and μ are in cm/s and mPa·s, respectively. It has been suggested by Ghannam and Esmail (1992) that the value of the critical speed of air entrainment is a strong function of the degree of dryness of a roller's surface before its re-entry in the liquid pool, where it is partially submerged in a horizontal

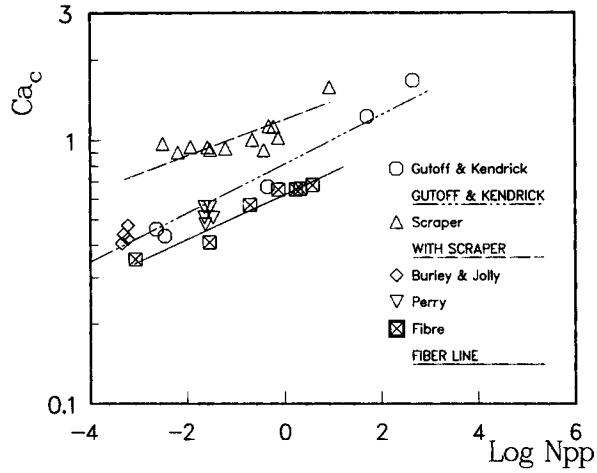

Figure 3. Dimensionless correlations of air entrainment.

position. In previous work, critical speeds were measured for rotating rollers under different conditions of dryness or wetness. Bolton and Middleman (1980) and Ghannam and Esmail (1992) measured the critical speeds for roller surfaces that were already covered by a thin layer of the same liquid as they re-entered the liquid pool. Wilkinson (1975) and Esmail and Ghannam (1990) applied scrapers to the roller surface before its re-entry, perhaps with different degrees of success in achieving a semidry condition. For the same viscosity, critical speed of air entrainment was highest in cases of surfaces that re-entered while covered by a thin liquid layer. Slightly lower values were those reported by Wilkinson (1975), and Esmail and Ghannam (1990) reported much lower values. Experiments with continuous dry tapes by Gutoff and Kendrick (1980) and Burley and Jolly (1984) gave the lowest critical air entrainment speeds for the same viscosity. Figure 2 shows that critical speeds measured for the continuous dry Monofilament fiber line agree well with previous results for continuous dry tapes. The conclusion is that although critical speed of air entrainment is a strong function of the degree of dryness or wetness of a surface before its wetting, for completely dry surfaces the critical speed is not influenced by the geometry (plane or cylindrical) of that surface.

In dimensionless form, the capillary *Ca*, Weber *We* and physical properties' N_{pp} numbers are the important parameter groups in the air entrainment phenomenon. Figure 3 shows the dimensionless correlation between the critical capillary number corresponding to the onset of air entrainment and the physical properties' number that defines the liquid phase. The regression correlation for experiments with the fiber line is:

$$Ca_c = 0.622\ N_{pp}^{0.085} \quad r = 0.95 \tag{5}$$

Comparison is made in Figure 3 with previous experiments by Gutoff and Kendrick (1980), Burley and Jolly (1984), Perry (1967) using continuous dry tapes, and with Esmail and Ghannam (1990) using a rotating roller with a scraper attached. Another useful regression correlation for the critical conditions of air entrainment in wetting of the fiber line, relates the critical values of the Weber number to the liquid properties' number

$$We_c = 0.311\ N_{pp}^{-0.462} \quad r = 0.97 \tag{6}$$

Equations 5 and 6 are useful in predicting the critical surface velocity of air entrainment as a function of the liquid properties.

Observations and measurements were made of the entrainment of air by the wetted fiber line when it plunges at different angles to the liquid surface. Using the stereoscopic microscope the circular contact line appeared horizontal and stable in the lower range of speeds. Depressions in this line appeared at the same time that tiny air bubbles were noticed in the liquid. The critical speed of the fiber was then recorded. Figure 4 shows these critical speeds. The angle α is measured from the liquid surface in one horizontal plane. Although the results show no significant changes in the critical speed with the angle α, a slight increase is consistently present for all tested liquids at the vertical position of the fiber line.

Fibers with four different diameters (Table 1) were used to study the effect of diameter on the critical speed of air en-

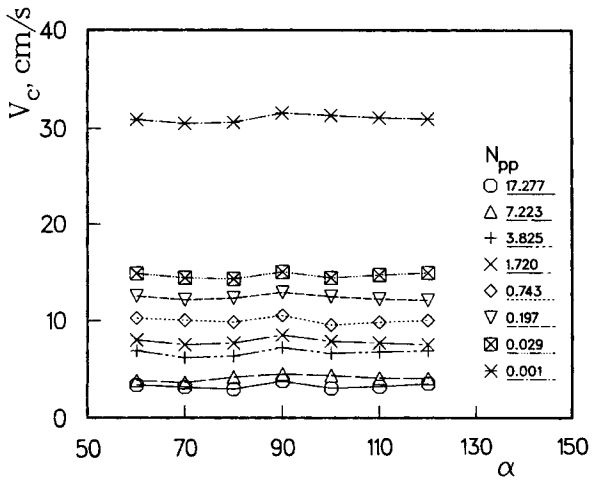

Figure 4. Effect of substrate entry angle on the critical air entrainment velocity.

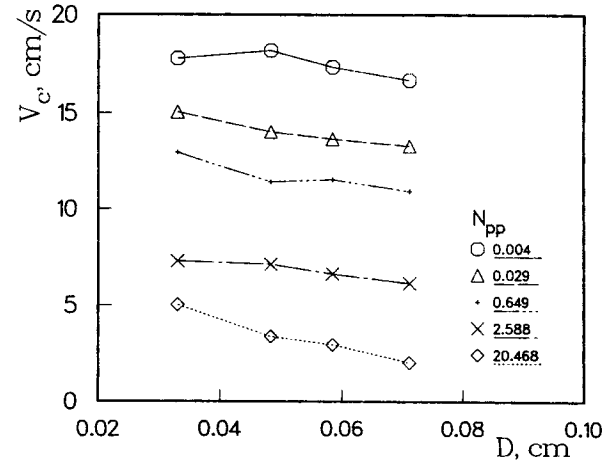

Figure 5. Effect of fiber line diameter on the critical air entrainment velocity.

trainment. Measurements were made for five glycerol solutions defined by values of physical properties' number ranging from $N_{pp} = 0.004$ to 20.468. The results are shown in Figure 5. A consistent decline in the critical speed of air entrainment was recorded for all tested solutions when the fiber diameter was increased. Gupta (1991) studied the dependence of critical speeds of air entrainment on surface tension coefficients. He used surfactants to vary the surface tension of glycerol solutions in wetting of continuous dry tapes. Consistent increase in the critical speed was observed with increase in the surface tension coefficient σ for all tested solutions. The critical speed increased more significantly for solutions with lower initial viscosity. An increase in fiber diameter in our experiments decreased the surface tension force that is dependent on the curvature as well as the surface tension coefficient. Therefore, we conclude that critical speeds of air entrainment increase or decrease with the surface tension force.

Notation

Bo = bond number ($\rho g L^2/\sigma$)
Ca = capillary number ($\mu V/\sigma$)
Ca_c = critical capillary number
D = fiber diameter, m
g = acceleration of gravity, m/s^2
L = characteristic length, m
L_c = capillary characteristic length $(\sigma/\rho g)^{0.5}$, m
L_d = Deryagin characteristic length $(\mu V/\rho g)^{0.5}$, m
N_{pp} = physical properties number ($g\mu^4/\rho\sigma^3$)
r = regression coefficient
Re = Reynolds number ($\rho VL/\mu$)
Re_c = critical Reynolds number
V = coating speed, m/s
V_c = critical coating speed, m/s
We = Weber number ($\rho V^2 L/\sigma$)
We_c = critical Weber number
W_{pp} = capillary diffusion velocity $(\mu/\rho)(\rho g/\sigma)^{0.5}$, m/s
X_d = interfacial displacement depth, m

Greek letters

α = substrate entry angle, degrees
θ = dynamic contact angle, degrees
θ_s = static contact angle, degrees
μ = viscosity, kg/m·s
ρ = density, kg/m^3
σ = surface tension, kg/s^2

Literature Cited

Blake, T. D., "Wetting Kinetics—How Do Wetting Lines Move?" AIChE Ann. Meet., New Orleans, paper 1a (Mar. 7-10, 1988).

Blake, T. D., and K. J. Ruschak, "A Maximum Speed of Wetting," *Nat.*, **282**, 489 (1979).

Bolton, B., and S. Middleman, "Air Entrainment in a Roll Coating System," *Chem. Eng. Sci.*, **35**, 597 (1980).

Burley, R., and B. S. Kennedy, "An Experimental Study of Air Entrainment at a Solid/Liquid/Gas Interface," *Chem. Eng. Sci.*, **31**, 901 (1976).

Burley, R., and R. P. S. Jolly, "Entrainment of Air Into Liquids by a High Speed Continuous Solid Surface," *Chem. Eng. Sci.*, **39**, 1357 (1984).

Esmail, M. N., and M. T. Ghannam, "Air Entrainment and Dynamic Contact Angles in Hydrodynamic of Liquid Coating," *Can. J. of Chem. Eng.*, **68**, 197 (1990).

Esmail, N. N., and R. L. Hummel, "Nonlinear Theory of Free Coating Onto a Vertical Surface," *AIChE J.*, **21**, 958 (1975).

Ghannam, M. T., "Air Entrainment and Dynamic Contact Angles in Hydrodynamics of Liquid Coating," PhD Thesis, University of Saskatchewan (1991).

Ghannam, M. T., and M. N. Esmail, "Effect of Substrate Entry Angle on Air Entrainment in Liquid Coating," *AIChE J.*, **36**, 1283 (1990).

Ghannam, M. T., and M. N. Esmail, "The Effect of Pre-wetting on Dynamic Contact Angles," *Can. J. of Chem. Eng.*, **70**, 408 (1992).

Gupta, R. K., "Air Entrainment Into Liquids by Continuous Flat Surfaces and the Effect of Surfactants," M.Sc. Thesis, University of Saskatchewan (1991).

Gutoff, E. B., and C. E. Kendrick, "Dynamic Contact Angles," *AIChE J.*, **28**, 459 (1982).

Perry, R. T., "Fluid Mechanics of Entrainment Through Liquid-Liquid and Liquid-Solid Junction," PhD Thesis, University of Minnesota (1967).

Rillaerts, E., and P. Joos, "The Dynamic Contact Angle," *Chem. Eng. Sci.*, **35**, 883 (1980).

Shames, I., "Mechanics of Fluids," McGraw-Hill, New York (1962).

Wilkinson, W. L., "Entrainment of Air by a Solid Surface Entering a Liquid/Air Interface," *Chem. Eng. Sci.*, **30**, 1227 (1975).

Manuscript received Nov. 13, 1991, and revision received June 15, 1992.